GEOPHYSICS, VOL. 55, NO. 10 (OCTOBER 1990); P. 1321–1326, 5 FIGS.

Inversion for magnetic anomalies of arbitrary three-dimensional bodies

X. Wang* and R. O. Hansen*

ABSTRACT

Two-dimensional (profile) inversion techniques for magnetic anomalies are widely used in exploration geophysics; but, until now, the three-dimensional (3-D) methods available have been restricted in their geologic applicability, dependent upon good initial values or limited by the capabilities of existing computers. We have developed a fully 3-D inversion algorithm intended for routine application to large data sets.

The algorithm, based on a Fourier transform expression for the magnetic field of homogeneous polyhedral bodies (Hansen and Wang, 1988), is a 3-D generalization of CompuDepth (O'Brien, 1972). Like CompuDepth, the new inversion algorithm employs the spatial equivalent of frequency-domain autoregression to determine a series of coefficients from which the depths and locations of polyhedral vertices are calculated by solving complex polynomials. These vertices are used to build a 3-D geologic model. Application to the Medicine Lake Volcano aeromagnetic anomaly resulted in a geologically reasonable model of the source.

INTRODUCTION

O'Brien (1972) described an approach (CompuDepth) to the magnetic inversion problem for two-dimensional (2-D) prismatic bodies. His algorithm is based on the fact that the Fourier transform of the horizontal derivative of the anomalous total magnetic field over a prismatic structure is a superposition of exponential functions. He used frequency shifting and Hilbert transforms to compute a set of data which form a set of simultaneous equations. By a spatial autoregression technique, the attenuation constants of the exponential functions (which are related to the depth of each edge) and the phase relationships (which determine the location of the edges of the sources) are determined. The results give the depth and location of each edge of the 2-D prismatic sources.

The inversion method presented in this paper is fundamentally an extension of CompuDepth to three dimensions, but it also incorporates elements from two other sources: Bhattacharyya and Leu's (1977) method of frequency-domain moments, extended to nth order; and Nabighian's (1984) generalized Hilbert transform, which appears raised to the nth power. This method is used to invert the total-field magnetic anomalies produced by multiple polyhedral source bodies over a regularly sampled surface. The method gives the coordinates of each vertex of the source bodies. These vertices can be used to build a three-dimensional (3-D) model, from which the geologic interpretation of the observed magnetic anomaly can be determined.

Like CompuDepth, this method does not need a guess for the initial values of the model. The only assumption for the application of the programs is that each source body can be approximated by a polyhedron and that it is homogeneously magnetized. By dividing the working area into small windows and working on one window at a time, this inversion method can work on large data sets.

The algorithm is presented in terms of total magnetic field anomalies. However, the modifications required for magnetic component or gravity anomalies are quite minor, since the technique relies only on the frequency-domain behavior of the anomaly. Using Pedersen's (1978) frequency-domain expressions for the transformation from one potential field to another, the necessary changes could be made easily.

FOURIER TRANSFORM EXPRESSION FOR THE MAGNETIC FIELD OF ARBITRARY 3-D BODIES

Every inversion algorithm used in potential field data processing is based on a forward model. The forward model for the inversion method presented in this paper is our frequency-domain expression for the magnetic field of arbitrary three-dimensional bodies (Hansen and Wang, 1988) which is a simplified form of Pedersen's (1978) formula. The formula is a sum of contributions of each vertex of the causative bodies and is in a coordinate-invariant form. For

Manuscript received by the Editor October 24, 1988; revised manuscript received April 9, 1990.
*Center for Potential Fields Studies, Department of Geophysics, Colorado School of Mines, Golden, CO 80401.

homogeneously magnetized polyhedral source bodies, the contribution of the jth vertex to the Fourier transform of the magnetic field is

$$\tilde{B}_{ej}(\mathbf{k}) = -2\pi \frac{1}{k} \frac{(\mathbf{K}\cdot\mathbf{J})(\mathbf{K}\cdot\mathbf{e})(\mathbf{m}_{j1}\times\mathbf{m}_{j2})\cdot\mathbf{m}_{j3}}{(\mathbf{K}\cdot\mathbf{m}_{j1})(\mathbf{K}\cdot\mathbf{m}_{j2})(\mathbf{K}\cdot\mathbf{m}_{j3})} E_j, \quad (1)$$

where

$\tilde{B}_{ej}$ = the portion of Fourier transform of the magnetic field contributed by vertex j, measured in the direction e;
$\mathbf{J}$ = the magnetization vector for the source body;
$\mathbf{k}$ = the wavenumber vector, $k = (k_x, k_y, 0)$;
k is the modulus of the wavenumber vector $\mathbf{k}$, $k = |\mathbf{k}|$;
$\mathbf{K} = (ik_x, ik_y, k)$;
$\mathbf{m}_{j1}, \mathbf{m}_{j2}, \mathbf{m}_{j3}$ = edge vectors from vertex j to its three adjacent vertices, arranged in right-handed order;
$E_j = \exp(-ik_x x_j - ik_y y_j - kz_j)$, where x_j, y_j, z_j are the coordinates of vertex j in the (x, y, z) system.

The magnetic field due to multiple source bodies is obtained by transforming the sum of the contributions of each vertex back to the spatial domain.

THE INVERSION ALGORITHM

The inversion algorithm for the positions and depths of vertices of the polyhedral source bodies is based on the fact that equation (1) is an exponential function of the vertex coordinates. Like CompuDepth (O'Brien, 1972), it computes the attenuation constants of the exponential functions (which are related to the depth of each vertex) and the phases (which determine the location of the vertices of the sources) through a spatial equivalent of autoregression.

The first step of the algorithm is to isolate the dependence of $\tilde{B}_{ej}(k)$ on the radial wavenumber k by defining

$$\mathbf{H} = \left(i\frac{k_x}{k}, i\frac{k_y}{k}, 1\right) = (i\cos\psi, i\sin\psi, 1), \quad (2)$$

where ψ is the angle from the k_x axis in the frequency domain. $\mathbf{H}$ is a vector whose first two components are just Nabighian's (1984) generalized Hilbert transform operator; note that it is independent of the radial wavenumber k.

The frequency-domain anomaly $\tilde{B}_{ej}(k)$ is then

$$\tilde{B}_{ej}(\mathbf{k}) = -2\pi \frac{1}{k^2} \frac{(\mathbf{e}\cdot\mathbf{H})(\mathbf{J}\cdot\mathbf{H})(\mathbf{m}_{j1}\times\mathbf{m}_{j2})\cdot\mathbf{m}_{j3}}{(\mathbf{m}_{j1}\cdot\mathbf{H})(\mathbf{m}_{j2}\cdot\mathbf{H})(\mathbf{m}_{j3}\cdot\mathbf{H})} \times \exp(-k\mathbf{H}\cdot\mathbf{r}_j). \quad (3)$$

Define $F_j = k^2\tilde{B}_{ej}$, the frequency-domain second vertical derivative of $\tilde{B}_{ej}(\mathbf{k})$, by

$$F_j(\mathbf{k}) = k^2\tilde{B}_{ej}(\mathbf{k}) = -2\pi \frac{(\mathbf{e}\cdot\mathbf{H})(\mathbf{J}\cdot\mathbf{H})(\mathbf{m}_{j1}\times\mathbf{m}_{j2})\cdot\mathbf{m}_{j3}}{(\mathbf{m}_{j1}\cdot\mathbf{H})(\mathbf{m}_{j2}\cdot\mathbf{H})(\mathbf{m}_{j3}\cdot\mathbf{H})} \times \exp(-k\mathbf{H}\cdot\mathbf{r}_j); \quad (4)$$

then the inward radial derivative of $\tilde{F}_j(\mathbf{k})$ is

$$\frac{\partial F_j}{\partial(-k)}(\mathbf{k}) = \delta_j F_j(\mathbf{k}), \quad (5)$$

where

$$\delta_j = \mathbf{H}\cdot\mathbf{r}_j, \quad (6)$$

and r_j is the position vector of vertex j,

$$\mathbf{r}_j = (x_j, y_j, z_j). \quad (7)$$

This result is essentially Bhattacharyya and Leu's (1977) moment relation generalized to arbitrary geometries.

Now consider an arbitrary collection of polyhedral bodies. Decomposing the magnetic field of these bodies into a sum over the n vertices of the bodies gives

$$F(\mathbf{k}) = \sum_{j=1}^{n} F_j(\mathbf{k}). \quad (8)$$

Applying equation (5) repeatedly gives

$$\frac{\partial^m F_j}{\partial(-k)^m}(\mathbf{k}) = \delta_j^m F_j(\mathbf{k}), \quad (9)$$

and therefore

$$\frac{\partial^n F}{\partial(-k)^n}(\mathbf{k}) = \sum_{j=1}^{n} \delta_j^n F_j(\mathbf{k}). \quad (10)$$

Define γ_m by

$$\sum_{m=0}^{n-1} \gamma_m \delta_j^m + \delta_j^n = 0. \quad (11)$$

This is a complex polynomial equation. For given values of $\delta_j, j = 1, 2, \ldots, n$, the coefficients $\gamma_m, m = 1, 2, \ldots, n-1$ can always be constructed so that equation (11) is satisfied. Equation (10) can be rewritten as

$$\begin{aligned}\frac{\partial^n F(\mathbf{k})}{\partial(-k)^n} &= \sum_{j=1}^{n} \delta_j^n F_j(\mathbf{k}) \\ &= -\sum_{j=1}^{n}\sum_{m=0}^{n-1} \gamma_m \delta_j^m F_j(\mathbf{k}) \\ &= -\sum_{j=1}^{n} \gamma_m \left[\sum_{m=0}^{n-1} \delta_j^m F_j(\mathbf{k})\right] \\ &= -\sum_{m=0}^{n-1} \gamma_m \frac{\partial^m F(\mathbf{k})}{\partial(-k)^m}. \end{aligned} \quad (12)$$

This result, which is a direct generalization (with some variations) of the autocorrelation equation of CompuDepth (O'Brien, 1972), is the fundamental relation for the algorithm.

The essence of the algorithm is as follows. Given anomalous field values, it is possible to calculate $F(\mathbf{k})$ and its first n inward radial derivatives. The autocorrelation equation (12) can then be solved for γ_m, $m = 0, 1, 2, \ldots, n$ along each ray in the (k_x, k_y) plane. Given the γ_m, the $\delta_j, j = 1, 2, \ldots, n$ are then determined by the polynomial equation (11) along each ray.

Two difficulties arise with the procedure just described. The first is that it would be necessary to solve for all vertex locations in an area simultaneously because of the superposition of anomalies in the frequency domain. This would be practical only if fairly small areas containing only a few anomalies could be used for the Fourier transform. In practice, relatively large areas are required for adequate low-frequency resolution. Thus, the number of vertices n will generally be impractically large. It is therefore necessary to find a version of equation (12) which is valid in the spatial domain, where anomaly separation is at least approximately possible.

The second difficulty is a consequence of the first. While the δ_j and γ_m are constant along each ray in the (k_x, k_y) plane, they vary with the angular coordinate ψ. To construct an inverse transform of equation (12), it is therefore necessary to find this angular dependence explicitly and to recast the equation in terms of unknown constants and quantities computable from $F(\mathbf{k})$. The strategy is to use the known (and fortunately simple) angular dependence of the δ_j to determine that of the γ_m using equation (11), and then to write equation (12) with the angular dependence explicit.

The relation giving the coefficients of a polynomial equation such as (11) in terms of its roots is well known:

$$\gamma_{n-m} = (-1)^m \sum_{j_1=1}^{n} \sum_{j_2=0}^{j_1-1} \cdots \sum_{j_m=1}^{j_{m-1}-1} \delta_{j_1}\delta_{j_2}\cdots\delta_{j_m}, \quad (13)$$

where $m = 1, 2, \ldots, n$.

Using this relation and the known angular dependence of the δ_j, an induction on the number of vertices n shows that the γ_m can be written in the form

$$\gamma_m = \sum_{p=0}^{n-m} \alpha_{m,p} i^p \cos p\psi + \beta_{m,p} i^p \sin p\psi, \quad (14)$$

where the $\alpha_{m,p}$ and $\beta_{m,p}$ are constants. Equation (12) can now be rewritten in the form

$$\frac{\partial^n F}{\partial(-k)^n}(\mathbf{k}) = -\sum_{m=0}^{n-1}\sum_{p=0}^{n-m}\left[\alpha_{m,p} i^p \cos p\psi \frac{\partial^m F}{\partial(-k)^m}(\mathbf{k}) + \beta_{m,p} i^p \sin p\psi \frac{\partial^m F}{\partial(-k)^m}(\mathbf{k})\right], \quad (15)$$

where the angular factors $i^p \cos p\psi$ and $i^p \sin p\psi$ are in essence the pth powers of Nabighian's (1984) generalized Hilbert transform operators. They have been grouped with the derivatives of F. These factors are used to operate on the Fourier transform of the observed data, yielding a correlation equation with constant coefficients.

Perform an inverse Fourier transform on equation (15) and define

$$A_{m,p} = \mathcal{F}^{-1}\left[i^p \cos p\psi \frac{\partial^m F(\mathbf{k})}{\partial(-k)^m}\right] \quad (16)$$

$$B_{m,p} = \mathcal{F}^{-1}\left[i^p \sin p\psi \frac{\partial^m F(\mathbf{k})}{\partial(-k)^m}\right]; \quad (17)$$

then the spatial-domain equivalent of equation (15) is

$$A_{n,0} = \sum_{m=0}^{n-1}\sum_{p=0}^{n-m} (\alpha_{m,p} A_{m,p} + \beta_{m,p} B_{m,p}). \quad (18)$$

This is a set of overdetermined simultaneous equations. The coefficients $A_{m,p}$ and $B_{m,p}$ are computable from equations (16) and (17). Then the unknown variables $\alpha_{m,p}$ and $\beta_{m,p}$ can be computed by using least-squares fitting to solve the simultaneous equations (18). From these $\alpha_{m,p}$ and $\beta_{m,p}$, we can form γ_m, $m = 0, 1, \ldots, n-1$, using equation (14).

Finally, we need to compute $\delta_j (j = 1, 2, \ldots, n)$ from the nth-order complex polynomial equation (11). Equation (11) has exactly n roots, as required for n vertices. From equations (2), (6), and (7) we have

$$\delta_j = \mathbf{H}\cdot\mathbf{r}_j = z_j + i(x_j \cos\psi + y_j \sin\psi). \quad (19)$$

It is obvious that equation (11) overdetermines the vertex coordinates shown in equation (19). For any two fixed values of ψ, a complete set of vertex locations can be calculated. This suggests attempting to solve equation (11) in a least-squares sense. However, a direct attack on this problem seems impractical, so an alternative strategy was devised. Since there are only a fixed number of coefficients $\alpha_{m,p}$ and $\beta_{m,p}$ for any number of vertices n, it is only necessary to solve equation (11) for a sufficient number of angles ψ to reflect the number of degrees of freedom in the system. The choices used are

$$\psi = 0, \frac{\pi}{2n}, \ldots, \frac{(2n-1)\pi}{2n}. \quad (20)$$

It is straightforward to verify that only values of ψ less than π lead to equations containing independent information.

The values of δ_j do not give (x_j, y_j, z_j) directly. The depth z_j is simply the real part of δ_j. To obtain x_j and y_j, write

$$\mu_j(\psi) = \mathrm{Im}\,\delta_j(\psi) = x_j \cos\psi + y_j \sin\psi. \quad (21)$$

Differentiating with respect to ψ yields

$$\mu_j'(\psi) = \nu_j(\psi) = -x_j \sin\psi + y_j \cos\psi. \quad (22)$$

Thus, if both $\mu_j(\psi)$ and $\nu_j(\psi)$ are known, x_j and y_j can be computed easily:

$$\begin{bmatrix} x_j \\ y_j \end{bmatrix} = \begin{bmatrix} \cos\psi & -\sin\psi \\ \sin\psi & \cos\psi \end{bmatrix}\begin{bmatrix} \mu_j(\psi) \\ \nu_j(\psi) \end{bmatrix}. \quad (23)$$

Differentiating the polynomial equation (11) with respect to ψ,

$$\sum_{m=0}^{n-1} \gamma'_m(\psi)\delta_j(\psi)$$

$$+\left[\sum_{m=1}^{n-1} k\gamma_m(\psi)\delta_j^{m-1}(\psi) + n\delta_j^{n-1}(\psi)\right]\delta'_j(\psi) = 0 \quad (24)$$

or

$$\delta'_j(\psi) = -\frac{\sum_{m=0}^{n-1} \gamma'_m(\psi)\delta_j^k(\psi)}{\sum_{\ell=1}^{n-1} \gamma_\ell(\psi)\delta_j^{\ell-1}(\psi) + n\delta_j^{n-1}(\psi)}. \quad (25)$$

Equation (25) gives the derivatives of $\delta_j(\psi)$ in terms of quantities which are known once the polynomial equation (11) has been solved. Substituting the imaginary part into equation (23) yields the coordinates x_j and y_j. The coordinates thus obtained for different values of ψ can then be averaged to give a final location estimate.

The flow chart of the inversion algorithm is shown in Figure 1.

INVERSION OF MEDICINE LAKE VOLCANO AEROMAGNETIC ANOMALY

The 3-D inversion method was used to determine the geometry of the source of the Medicine Lake Volcano aeromagnetic anomaly. Comparison of the results with the model obtained by Evans and Zucca (1988) provides a test of the inversion method on real data.

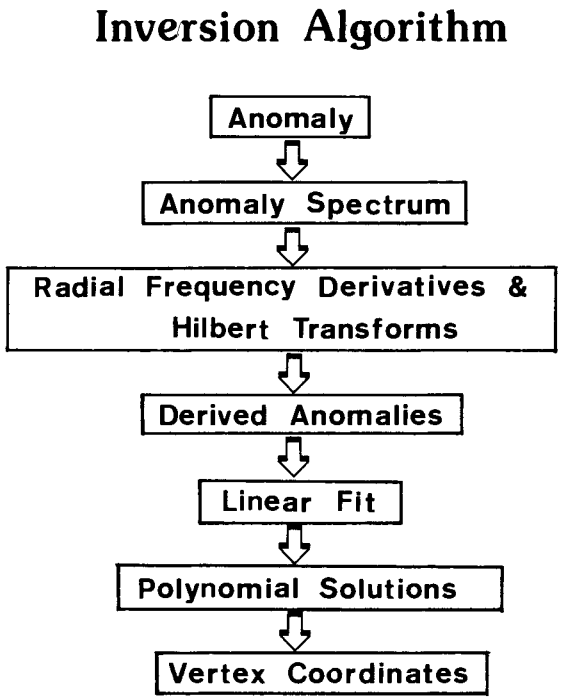

FIG. 1. Flow chart of the inversion algorithm.

Oregon State University conducted an aeromagnetic survey in the area between 40°15′ and 42°15′ N latitude and 120°45′ and 122°45′ W longitude in northern California (Huppunen, 1983), which includes the Medicine Lake Volcano. Figure 2 shows the total field aeromagnetic map of that area, which covers an area of 51 by 41 km at a grid spacing of 1 km. On this map, Medicine Lake Volcano is associated with a positive anomaly surrounded by negative values. The maximum amplitude of the positive anomaly is about 1200 nT and that of the negative values is about −1000 nT.

The Medicine Lake Volcano, a shield with a central caldera, has erupted basalt, andesite, dacite, and rhyolite over a period of about 1 m.y. (Anderson, 1941; Mertzman, 1981; Donnelly-Nolan, 1988). These rocks are called the High Cascade sequence. Older, probably Tertiary to early Pleistocene, basalts are exposed in fault scarps (Donnelly-Nolan et al., 1981) and appear to make up a 2 to 3 km thick volcanic layer that partially underlies the flanks of the volcano (LaFehr, 1965; Stanley, 1982). These rocks are called the Western Cascade sequence.

Finn (1981) and Finn and Spydell (1982) conducted a detailed gravity survey in this area and found a gravity high over the Medicine Lake Volcano. Finn and Williams (1982) modeled the gravity data with a shallow intrusive complex in the upper crust that is 0.4 g/cm^3 denser than surrounding rocks. This interpretation is supported by the electromagnetic sounding work of Stanley (1982). Evans and Zucca (1988) performed a seismic tomographic study of the area and gave a detailed cross-section of the Medicine Lake Volcano (Figure 3) based on their inversion.

The results of applying the inversion algorithm to the Medicine Lake Volcano aeromagnetic anomaly are shown in Figure 4. A total of 87 depth points computed by the inversion are shown on this map; the depths range from 0.10 to 9.02 km.

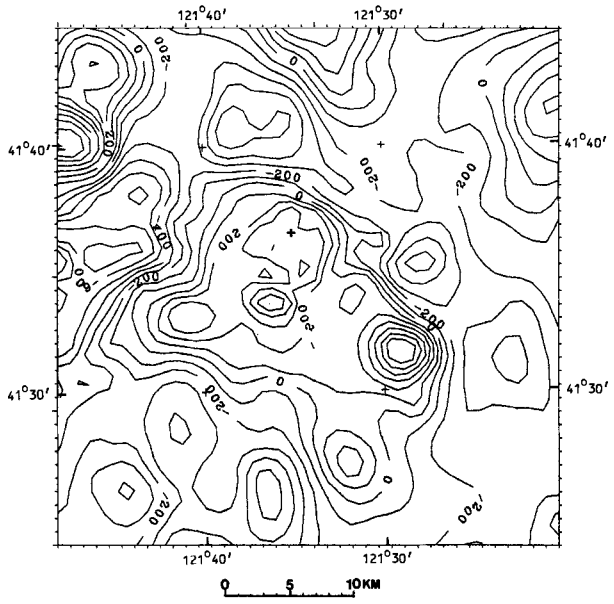

FIG. 2. Aeromagnetic anomaly map of the Medicine Lake Highland area. Contour interval = 100 nT. The + indicates Medicine Lake.

Figure 4 illustrates clearly the distinction between an inversion of the data and a geologic interpretation. Our algorithm computes vertex locations and depths based on a multipolyhedral model, not geologic structure. The results may then be interpreted geologically, but in complex environments such as the Medicine Lake Volcano this is far from a trivial task. The problem of inferring the geologic structure from the inversion results is not unique to our algorithm; it occurs also in many 2-D inversion programs. However, for a 3-D inversion the difficulties are greatly increased by problems in properly visualizing the results. This is an area in which we plan further research.

The complexity of the structures implied by the depth estimates in Figure 4 has thus far stymied attempts at a complete interpretation. However, the cross-section AA' matches the geologic model of Evans and Zucca (1988) (Figure 3). The result of projecting the nearby depth estimates from Figure 4 onto the section and superimposing the estimates on Evans and Zucca's model is shown in Figure 5. In Figure 5, the depth estimates appear as solid dots and the interpreted bodies as dashed lines.

With the geologic model as a guide, the significance of the inversion results is clear. One set of depth estimates outlines the topography with reasonable accuracy. A second set matches the outline of the interpreted intrusion with remarkable fidelity. As one would expect, there are few points associated with the lower surface of the intrusion, and these are near the edges.

This leaves two depth estimates, both located inside but near the top of the magma chamber interpreted by Evans and Zucca (1988) from the presence of a low-velocity zone. However, they note in their figure caption for the section that the magma chamber may be smaller than indicated. Our inversion results suggest that this is indeed the case, and we tentatively identify these two depth estimates as associated with the Curie transition above the magma chamber.

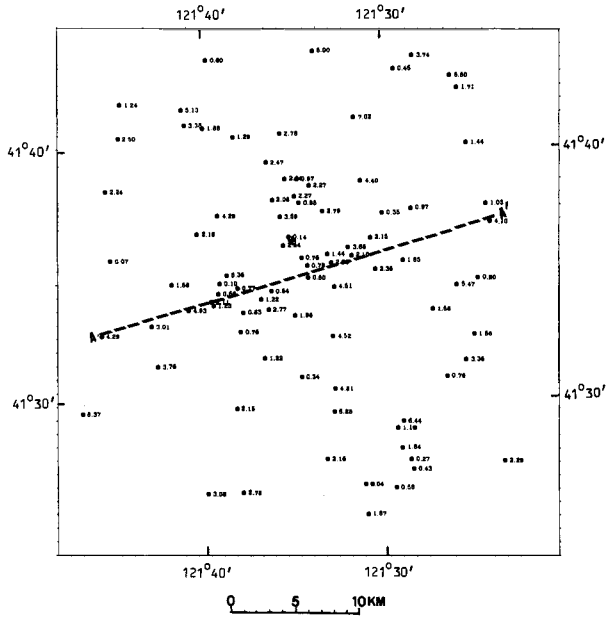

FIG. 4. The result of inversion of the Medicine Lake Highland aeromagnetic anomalies. Spotted values are depths in km below the flight elevation; the cross is at the location of Medicine Lake. AA' indicates the profile shown in Figure 5.

Obviously, the single section presented in Figure 5 does not exhaust the information shown in Figure 4. However, it does demonstrate that our inversion algorithm can yield geologically intelligible results. With improved presentation and ancillary information such as error estimates, susceptibility contrasts, and dip angles that the program can be modified to provide, we expect to be able to extract much more information from the inversion results and hope to obtain much more complete interpretations.

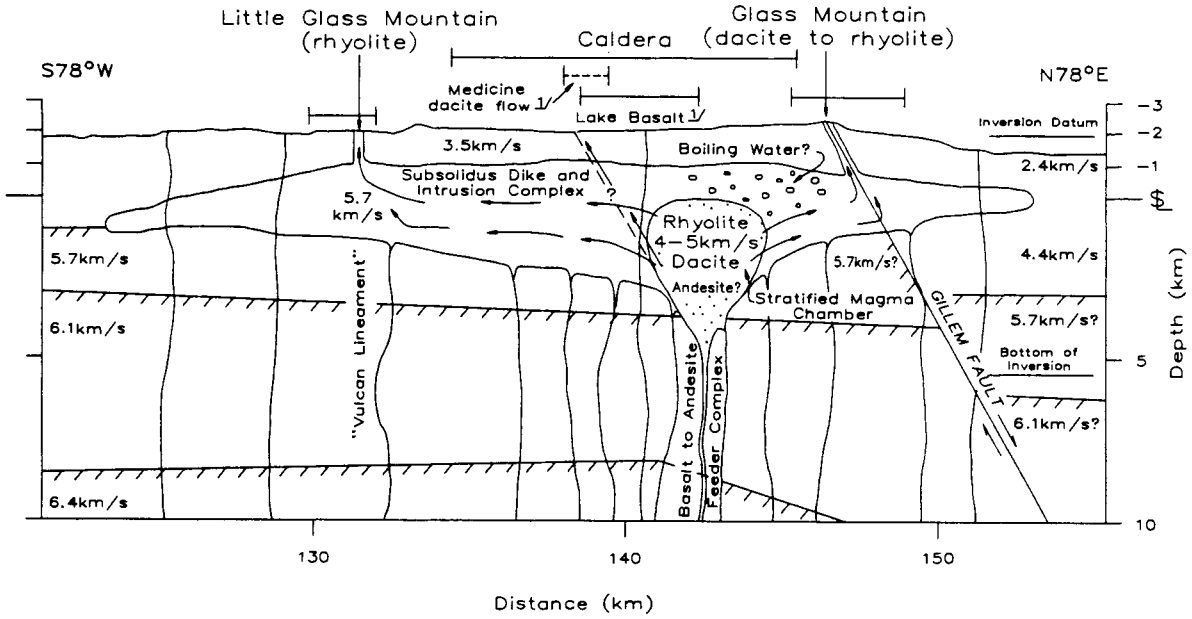

FIG. 3. Geologic model of the Medicine Lake Volcano obtained from seismic tomography (Evans and Zucca, 1988).

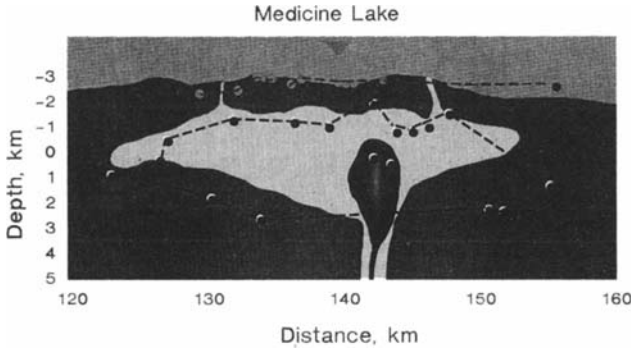

FIG. 5. Comparison of the model obtained by inversion with the model from seismic tomography along the profile AA′ of Figure 4. The light stippled area indicates the intrusive body, the dark area within it the inferred magma chamber. The dots are at the projected locations of the depth estimates near the line.

CONCLUSIONS

This paper presents a 3-D inversion method which promises to be an efficient technique for geologic interpretation of magnetic anomalies due to arbitrary distribution of source bodies. The inversion of the aeromagnetic data from the Medicine Lake Volcano shows that the algorithm can be used to obtain a geologically reasonable interpretation of aeromagnetic anomalies in a very complex geologic environment.

While we believe that the work presented here establishes the validity and potential usefulness of the inversion algorithm, much remains to be done to produce a routinely usable interpretation tool. The problems are well illustrated by Figure 5: a collection of depth estimates does not constitute an interpretation of the data. Although in this instance the existence of an interpreted geologic section enabled us to match a portion of the results with established geologic structures, such a procedure is obviously unsatisfactory in general. We therefore plan to investigate techniques for displaying and organizing the inversion results to facilitate their interpretation.

ACKNOWLEDGMENTS

We wish to thank the sponsors of the Center for Potential Fields Studies for their continuing support and encouragement, Norman Harthill for his assistance in interpreting the Medicine Lake Highland results, and Hengren Xia for providing background information on the geology and geophysics of the Cascades. We also thank the reviewers of the paper for helpful comments and for supplying some additional references.

REFERENCES

Anderson, C. A., 1941, Volcanoes of the Medicine Lake Highland, California: Univ. of California Publications, Department of Geological Sciences, Bulletin, **25**, 347–422.

Bhattacharyya, B. K., and Leu, L.-K., 1977, Spectral analysis of gravity and magnetic anomalies due to rectangular prismatic bodies: Geophysics, **42**, 41–50.

Donnelly-Nolan, J. M., Ciancanelli, E. V., Eichelberger, J. C., Fink, J. H., and Heiken, G., 1981, Roadlog for field trip to Medicine Lake Highland, *in* Johnston, D. A., and Donnelly-Nolan, J., Eds., Guides to some volcanic terranes in Washington, Idaho, Oregon, and Northern California: U.S.G.S. Circular 838, 141–149.

Donelly-Nolan, J. M., 1988, A magmatic model of Medicine Lake Volcano, California: J. Geophys. Res., **93**, 4412–4420.

Evans, J. R., and Zucca, J. J., 1988, Active high-resolution seismic tomography of compressional wave velocity and attenuation structure at Medicine Lake Volcano, northern California Cascade Range: J. Geophys. Res., **93**, 15016–15036.

Finn, C., 1981, Complete Bouguer map of Medicine Lake, California, 15′ topographic quadrangle: U.S.G.S. Open-file rep. 1-0098.

Finn, C., and Spydell, D. R., 1982, Principal facts for seventy-four gravity stations in the northern California Cascade mountains: U.S.G.S. Open-file rep. 82-1080.

Finn, C., and Williams, D. L., 1982, Gravity evidence for a shallow intrusion under the Medicine Lake volcano, California: Preliminary results: Geology, **10**, 503–507.

Hansen, R. O., and Wang, X., 1988, Simplified frequency-domain expressions for potential fields of arbitrary three-dimensional bodies: Geophysics, **58**, 365–374.

Huppunen, J. L., 1983, Analysis and interpretation of magnetic anomalies observed in north-central California: Ph.D. thesis, Oregon State Univ.

LaFehr, T. R., 1965, Gravity, isostasy, and crustal structure in the southern Cascade Range: J. Geophys. Res., **70**, 5581–5597.

Mertzman, S. A., Jr., 1981, Pre-Holocene silicic volcanism in the northern and western margins of the Medicine Lake volcano, California, *in* Johnston, D. A., and Donnelly-Nolan, J., eds., Guides to some volcanic terranes in Washington, Idaho, Oregon, and Northern California: U.S.G.S. Circular 838, 163–169.

Nabighian, M. N., 1984, Toward a three-dimensional automatic interpretation of potential field data via generalized Hilbert transforms: Fundamental relations: Geophysics, **49**, 780–786.

O'Brien, D. P., 1972, CompuDepth—A new method for depth-to-basement calculation: Presented at the 42nd Ann. Internat. Mtg., Soc. Expl. Geophys., Anaheim.

Pedersen, L. B., 1978, Wavenumber domain expressions for potential fields from arbitrary 2, 2 1/2, and 3-dimensional bodies: Geophysics, **43**, 626–630.

Stanley, W. D., 1982, A regional magnetotelluric survey of the Cascade Mountains region: U.S.G.S. open-file rep. 82-126.